ChemComm

Accepted Manuscript

ROYAL SOCIETY OF CHEMISTRY

rsc.li/chemcomm

View Article Online
DOI: 10.1039/C8CC05069D

Journal Name

COMMUNICATION

Fine-Tuning the Assemblies of Carbon Nanodots and Porphyrins†

Tobias Scharl,[a] Alejandro Cadranel,[a] Phillip Haines,[a] Volker Strauss,[a] Sarah Bernhardt,[a] Sonia Vela,[b] Carmen Atienza,[b] Franziska Gröhn,[a] Nazario Martín,*[b] and Dirk M. Guldi.*[a]

Received 00th January 20xx,
Accepted 00th January 20xx

DOI: 10.1039/x0xx00000x

www.rsc.org/

We present charge-transfer assemblies of electron accepting, pressure-synthesized carbon nanodots (pCNDs) and an electron donating porphyrin. Amidine derivatization of the porphyrin allows for hydrogen bonding interactions with the carboxyl groups in the surface of pCNDs, which drive the formation of the assembly. Upon photoexcitation, this electron donor-acceptor supramolecular construct features ultrafast charge separation, and subsequent charge recombination in 27 ps.

The quest for novel energy conversion and energy storage schemes by means of renewable sources is drawing increasing attention across the scientific disciplines. At the forefront of energy conversion schemes is the design of molecular systems and materials that ultimately perform light harvesting and charge transfer both with high efficiency. Aspects such as low production costs and biocompatibility govern the criteria, which would eventually enable the securing of sustainable solutions for replacing the carbon-based energy matrix.

One class of material, namely synthetic carbon allotropes, in general, and carbon nanodots (CND), in particular, meets all of the aforementioned criteria.[1] CNDs are known for their remarkable physicochemical properties, which includes strong and medium-dependent photoluminescence.[2] The electronic structure of CNDs is well-balanced so that they function both as electron donors and acceptors, providing them with an amphoteric redox behavior. The structure of CNDs depends, however, largely on the respective starting materials and preparation method. For example, pressure-synthesized CNDs[3] (**pCND**) possess a very interesting, yet not completely deciphered structure. **pCND**s are best-described in terms of a conjugated core and a poly-functional, amorphous surface rich in carboxyl groups. Considering such a multi-faceted nature, different approaches to couple complementary electron donors or acceptors to **pCND**s seem feasible. For example, electrostatics and/or π-stacking interactions were exploited to design **pCND**-based electron donor-acceptor assemblies in combination with perylene bisimides (PDI) and single-walled carbon nanotubes (SWCNT).[4,5]

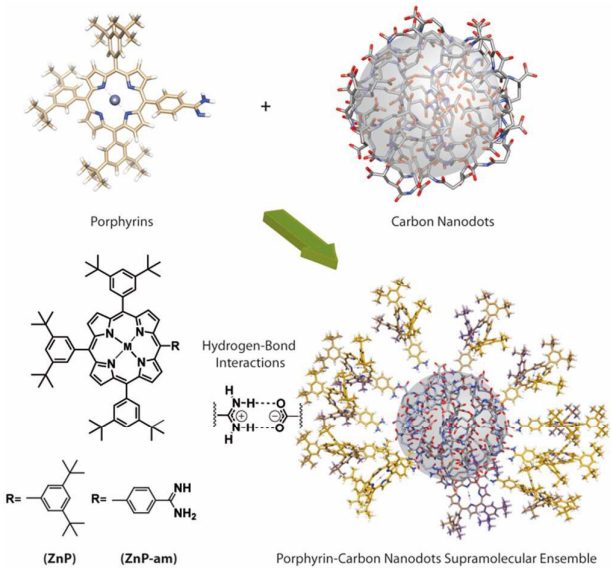

Scheme 1. Up: Representation of the porphyrin and **pCND**s prepared endowed with amidine and carboxyl groups, respectively. Down: Sketches of the porphyrins studied in this work, that is, **ZnP-am** and **ZnP**, and the final electron donor-acceptor supramolecular construct formed from the amidinium-carboxylate salt-bridge based on hydrogen-bond interactions.

In energy conversion schemes, the control over inter-component interactions is of utmost importance. On one hand, energy and/or electron donors and acceptors are easily

[a] Department of Chemistry and Pharmacy & Interdisciplinary Center for Molecular Materials (ICMM), Friedrich-Alexander Universität Erlangen-Nürnberg, Egerlandstr. 3, 91058 Erlangen, Germany.
[b] Department of Organic Chemistry, Faculty of Chemistry, University Complutense of Madrid, Avenida Complutense s/n, Ciudad Universitaria, Madrid, Spain.

†Electronic Supplementary Information (ESI) available: Titrations of **pCND/ZnP** mixtures, Stern-Volmer plots for porphyrin emission quenching, electrochemical titration of **pCND/ZnP-am**, transient absorption spectroscopy of **ZnP-am**, spectroelectrochemistry for **ZnP-am**, and tables with the time constants extracted from target analyses. See DOI: 10.1039/x0xx00000x

View Article Online
DOI: 10.1039/C8CC05069D

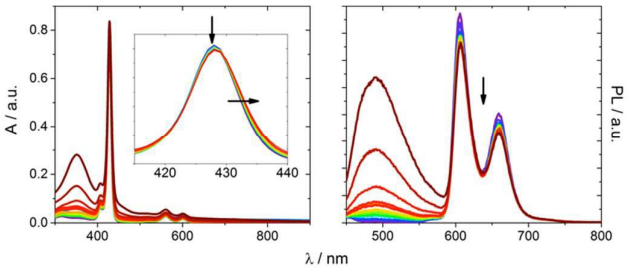

Figure 1. Absorption (left) and fluorescence (right) spectra of ZnP-am (purple, 2 × 10-6 M) throughout the course of a titration with **pCNDs** (blue to dark red) in anhydrous DMF at room temperature (λ_{ex} = 420 nm). Final spectra corresponds to a [**pCND**] of 10 mg/L. Inset: Intensity decrease and red-shift of the Soret absorption band.

assembled by means of covalent bridges, which enable spatial control in the final arrangement. Notably, covalent modification of the individual components may significantly alter their electronic structure and, in turn, impact the energy and/or electron transduction. On the other hand, hydrogen bonding interactions, which are omnipresent in the natural photosynthetic systems,[6-8] constitute a promising alternative. When compared to other non-covalent interactions, such as electrostatics or π-stacking, hydrogen bonding is more specific and directional.[9] As such, it guarantees far better-defined architectures.

It is in living organisms, where guanidinium-carboxylate salt bridges promote considerable electronic coupling between the individual components and control over the dynamics and efficiencies of energy and/or electron transfer processes.[10-13] In artificial models, amidinium-carboxylate rather than guanidinium-carboxylate salt bridges (Scheme 1) enable an even higher level of specificity. As a matter of fact, amidinium-carboxylate salt bridges in electron donor-acceptor systems reinforce, on one hand, the strength of the hydrogen-bonding network and ensures, on the other hand, an efficient charge transport from one electroactive terminus to another.[14-15]

Porphyrins have emerged as an ideal complement to **pCND**s both in terms of light harvesting and charge transfer. In fact, their intense absorptivity and their remarkable electron donating character have already been corroborated in covalent conjugates with nitrogen-rich CNDs.[16] In this contribution, we explore hydrogen bonding interactions between an amidine-functionalized porphyrin[17] (**ZnP-am**, Scheme 1) and the carboxylic acids on the surface of **pCND**s to afford salt-bridges between them. In particular, we probed **pCND**s together with **ZnP-am** by means of steady-state and time-resolved spectroscopy techniques.

pCNDs and **ZnP-am** were prepared as previously described.[3,18] Ground state interactions were studied by means of steady state spectrophotometric absorption titration assays in anhydrous DMF. Significant changes evolve in the absorption spectrum of **ZnP-am** upon addition of **pCND**s (Figure 1). Overall, the Soret-band absorption decreases and slightly red-shifts resulting in isosbestic points at 420 and 430 nm. This finding is in stark contrast to the results obtained for the **ZnP** reference, where in analogous titrations only overlapped absorption features stemming from the individual components were noted (Figure S1). At this point we postulate the presence of charge transfer (CT) interactions in the form of **(ZnP-am)$^{+}$•(pCND)$^{-}$**.

Independent proof for the **ZnP-am•pCND** formation came from dynamic light scattering (DLS) measurements – Figures S4 and S5. Beside larger particles, DLS measurements of **pCND** revealed a hydrodynamic radius (R_H) around of 0.65 ± 0.42 nm, while **ZnP-am•pCND** exhibited a hydrodynamic radius around 0.93 ± 0.34 nm.[§]

Additional confirmation for sizable ground state CT interactions in **ZnP-am•pCND** came from electrochemical measurements. Square-wave voltammetry measurements (SWV) were performed for the individual components (**ZnP-am** and **pCND**s) and the final supramolecular ensemble (**ZnP-am•pCND**s) at room temperature and using anhydrous DMF. **ZnP-am** exhibits an oxidation at +0.91 V – Figure S6 – meanwhile, the first and second reduction of **pCND**s appear at -0.59 and -0.94 V[19]. From these data, we obtain the lowest charge-separated state energies of 1.50 eV for **ZnP-am•pCND**s. Upon addition of **pCND**, the oxidation of **ZnP-am** shifts anodically to 1.11 V –Figure S6. Implicit is a shift of electron density from the electron donating **ZnP-am** to the electron accepting **pCND**, which, in turn, renders the **ZnP-am** in **(ZnP-am)$^{+}$•(pCND)$^{-}$** oxidation more difficult.

Complementary fluorescence titrations allowed analyzing excited state interactions. Most notable is the fact that the **ZnP-am** centered fluorescence is quenched in the presence of **pCND**s using 420 nm as excitation wavelength – Figure 1, resulting in a Stern-Volmer constant of 0.088 mg^{-1}L – Figure S2. This value is comparable to those found for electrostatically assembled **(ZnP^{4+})•pCND** (0.083 mg^{-1}L).[20] Overall, maximum fluorescence quenching is noted in the range of 15% when amounts of up to 10 mg/L **pCND**s are present – Figure S3.[‡] In reference experiments with **ZnP** – lacking the amidine functionality – the quenching is far below 5% and reflects only contributions from π-stacking interactions.

In short, the addition of **pCND**s to **ZnP-am** activates in the resulting **ZnP-am•pCND** additional decay channels, which are absent for **ZnP-am**. To corroborate that photoinduced charge separation, which is a thermodynamically downhill process from the second singlet excited state (S_2) and the first singlet excited state (S_1) of **ZnP-am** with 2.90 and 2.07 eV, respectively, takes place rather than any other deactivation, femtosecond pump-probe experiments were performed with **ZnP-am** and its mixtures with **pCND**s in anhydrous DMF. Selective excitation into the porphyrin' Soret-band absorption was realized by using a 420 nm (2.95 eV) pump.

With the help of Global analyses the number of intermediate states, which participate in the decay cascades, were determined together with their lifetimes and decay associated spectra.[21-23] For example, the excited state dynamics of **ZnP-am** are best fit by a four species model – Figure S7. Right after photoexcitation, the second singlet excited state (S_2) is populated, which features maxima at 457, 586, and 642 nm together with minima at 564 and 603 nm. In 1.9 ps, internal conversion populates the first singlet excited state (S_1), for which similar maxima and minima are noted. From there on, it

View Article Online
DOI: 10.1039/C8CC05069D

is a 1.8 ns intersystem crossing, which yields the microsecond decaying triplet excited state (T_1), and, which reinstates the ground state (GS). Characteristics of T_1 are 474, 586, and 645 nm maxima.[§§]

ZnP-am shows changes in its excited state dynamics when **pCND**s are present. For **ZnP-am•pCND**, the (**ZnP-am**)$^{+}$•(**pCND**)$^{-}$ CT state with its 470, 587, and 640 nm maxima and 564 and 604 nm minima is initially populated – Figure 2. This CT state transforms in parallel to S_1 and a new state. In the context of the earlier, the following maxima and minima testify the formation of S_1: 590 / 638 nm and 563 / 605 nm, respectively.[§§§]

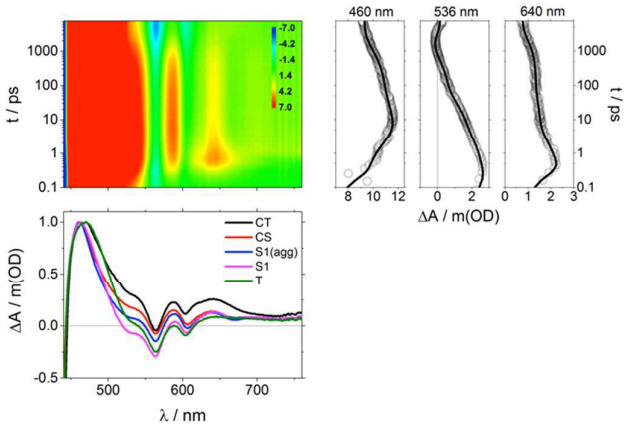

Figure 2. Upper left: Differential absorption 3D map obtained upon femtosecond pump-probe experiments (λ_{ex} = 420 nm) of **ZnP-am•pCND** in anhydrous DMF at room temperature. Upper right: Time absorption profiles (open circles) and global analysis fittings (solid lines). Bottom left: Normalized decay associated spectra: S2, black; CS, red; S1(agg), blue; S1, magenta; T, green.

For the latter, the decay associated spectrum reveals enhanced photoinduced absorptions in the range around 640 nm. In line with the spectroelectrochemical generation of the one-electron oxidized (**ZnP-am**)$^{\bullet+}$ – Figure S8 – which match the current observation, we postulate the formation of the (**ZnP-am**)$^{\bullet+}$•(**pCND**)$^{\bullet-}$ charge-separated state. Interestingly, charge recombination takes place within 27 ps, a lifetime in the range found for charge-separated states in related electrostatically assembled carbon nanodot / porphyrins systems. Our interpretation is consistent with the coexistence of **ZnP-am•pCND** and **ZnP-am**. This goes hand-in-hand with the moderate quenching of the porphyrin fluorescence – vide supra.

In conclusion, a new approach for assembling electron donor-acceptor ensembles based on **pCNDs** and porphyrins has been explored: amidinium-carboxylate salt bridges. Overall, the electron accepting properties of **pCNDs** are well complemented by the electron donating properties of porphyrins. This results in CT interactions in the ground state and charge separation in the excited state.

AC acknowledges a DAAD/ALEARG postdoctoral fellowship and is a member of ALN. This work was supported by the Deutsche Forschungsgemeinschaft (DFG) via SFB 953 "Synthetic Carbon Allotropes". NML acknowledges support from the European Research Council (ERC-320441-Chirallcarbon), the MINECO of Spain (project CTQ2014-52045-R) and the Comunidad de Madrid (PHOTOCARBON project S2013/MIT-2841). C.A thanks to the Ramón y Cajal grant.

Conflicts of interest

There are no conflicts to declare.

Notes and references

‡ The usage of hydrous rather than anhydrous DMF eliminates the fluorescence quenching of **ZnP-am**. Water interferes with the corresponding hydrogen bonding interactions between **ZnP-am** and **pCND**s.

§ The standard deviations of the particle size distributions are σ = 0.08 and 0.36 for the **pCND**s and **ZnP-am•pCND**, respectively – Table S1. Assuming a same density of the coexisting particles, the volume-weighted size distributions show that more that 90% of the pCNDs are present as individual particles and 0.3% to 8% in the form of larger aggregates.

§§ The presence of an additional 229 ps component is ascribed to fast decaying aggregates of the porphyrins to GS.

§§§ Once formed, S_1 intersystem-crosses in 1.3 ns to the microsecond-lived T_1 next to an aggregated form of S_1.

1 Strauss, V.; Roth, A.; Sekita, M.; Guldi, D.M. *Chem*., 2016, **1**, 531-556.
2 Baker, S. N.; Baker, G. A. *Angew. Chem. Int. Ed.*, 2010, **49**, 6726 – 6744.
3 Strauss, V.; Margraf, J. T.; Dolle, C.; Butz, B.; Nacken, T. J.; Walter, J.; Bauer, W.; Peukert, W.; Spiecker, E.; Clark, T.; Guldi, D. M. *J. Am. Chem. Soc.*, 2014, **136**, 17308-171316.
4 Strauss, V.; Margraf, J. T.; Clark, T.; Guldi, D. M. *Chem. Sci.*, 2015, **6**, 6878-6885.
5 Strauss, V.; Margraf, J. T.; Dirian, K.; Syrgiannis, Z.; Prato, M.; Wessendorf, C.; Hirsch, A.; Clark, T.; Guldi, D. M. *Angew. Chem. Int. Ed.*, 2015, **54**, 8292-8297.
6 Guldi, D. M.; Martín, N. *J. Mater. Chem.,* 2002*, **12**,* 1978-1992.
7 Uyeda, G.; Williams, J. C.; Roman, M.; Mattioli, T. A.; Allen, J.P. *Biochemistry*, 2010, **49**, 1146–1159.
8 Polander, B. C.; Barry, B. A., *J. Phys. Chem. Lett*., 2013, **4**, 786–791.
9 Sánchez, L.; Martín, N.; Guldi, D. M. *Angew. Chem. Int. Ed.*, 2005, **34**, 5374-5382.
10 Wenger, O. S. *Chem. Eur. J.*, 2011, **17**, 11692 – 11702.
11 Deng, Y.; Roberts, J. A.; Peng, S-M.; Chang, C. K.; Nocera, D. G. *Angew. Chem. Int. Ed.*, 1997, **36**, 2124-2127.
12 Sánchez, L.; Sierra, M.; Martín, N.; Myles, A. J.; Dale, T. J.; Rebek, J.; Seitz, Jr.W.; Guldi, D. M. *Angew. Chem. Int. Ed.*, 2006, **45**, 4637-4641
13 Vela, S; Bauroth, S.; Atienza, C.; Molina-Ontoria, A.; Guldi, D.M.; Martín, N. *Angew. Chem. Int. Ed.*, 2016, **55**, 15076-15080
14 Kirby, J. P.; Roberts, J. A.; Nocera, D. G. *J. Am. Chem. Soc.*, 1997, **119**, 9230 – 9236
15 Damrauer, N. H.; Hodgkiss, J. M.; Rosenthal, J.; Nocera, D. G. *J. Phys. Chem. B*, 2004, **108**, 6315 – 6321.
16 Arcudi, F.; Strauss, V.; Dordevic, L.; Cadranel, A.; Guldi, D.M; Prato, M. *Angew. Chem. Int. Ed.*, 2017, **129**, 12265 –12269.
17 Otsuki, J.; Iwasski, K.; Nakano, Y.; Itou, M.; Araki, Y.; Ito, O. *Chem. Eur. J.*, 2004, ***10***, 3461-3466.
18 Otsuki,J.; Iwasaki, K.; Nakano, Y.; Itou, M.; Araki, Y.; Ito, O. *Chem.Eur.J.*, 2004, **10**, 3461-3466.
19 Strauss, V.; Kahnt, A.; Zolnhofer, E.; Meyer, K.; Maid, H.; Placht, C.; Bauer, W.; Nacken, T. J.; Peukert, W.; Etschel, S.

View Article Online
DOI: 10.1039/C8CC05069D

H.; Halik, M.; Guldi, D. M. *Adv. Funct. Mater.*, 2016, **26**, 7975-7985.
20 Cadranel, A.; Strauss, V.; Margraf, J. T.; Winterfield, K.; Vogl, C.; Đorđević, L.; Arcudi, F.; Hoelzel, H.; Jux, N.; Prato, M.; Guldi, D. M. *J. Am. Chem. Soc.*, 2018, **140**, 904-907.
21 Van Stokkum, I. H. M.; Larsen, D. S.; Van Grondelle, R. *Biochim. Biophys. Acta, Bioenerg.*, 2004, **1657**, 82-104.
22 van Wilderen, L. J. G. W.; Lincoln, C. N.; van Thor, J. J. *PLoS One*, 2011, **6(3)**, e17373.
23 Snellenburg, J.J.; Laptenok, S. P.; Seger, R.; Mullen, K. M.; van Stokkum, I. H. M.; *J. Stat. Soft.*, 2012, **49(3)**, 1–22.